Journal of Molecular Graphics and Modelling 39 (2013) 13–22

Contents lists available at SciVerse ScienceDirect

Journal of Molecular Graphics and Modelling

journal homepage: www.elsevier.com/locate/JMGM

Structural analysis of the inhibition of APRIL by TACI and BCMA through molecular dynamics simulations

Maite González-Mendióroz, Ana Belén Álvarez-Vázquez, Jaime Rubio-Martinez*

Department of Physical Chemistry, University of Barcelona and the Institut de Recerca en Quimica Teorica i Computacional (IQTCUB), Barcelona, Spain

ARTICLE INFO

Article history:
Received 18 August 2012
Received in revised form 4 November 2012
Accepted 5 November 2012
Available online 17 November 2012

Keywords:
APRIL
TACI
BCMA
Drug design
Tumour necrosis factor
Molecular dynamics

ABSTRACT

APRIL (a proliferation-inducing ligand) is a member of the tumour necrosis factor (TNF) superfamily that binds the receptors (TNFRs) TACI and BCMA. Since it was discovered, a great amount of evidence has been reported about the involvement of APRIL in autoimmune diseases including systemic lupus erythematosus (SLE), rheumatoid arthritis (RA), Sjögren's syndrome (SS) and multiple sclerosis (MS). In addition, an important role of APRIL has been described in different types of tumour cell lines and in a variety of primary tumour tissues where, in contrast with the normal ones, high mRNA levels have been detected. Accordingly, the design of compounds mimicking the inhibition of APRIL by its receptors appears to be a promising way to treat autoimmune and cancer diseases. As a first step to achieve these goals and in order to better understand the key interactions involved in these systems, we report a structural analysis of the inhibition of human and murine APRIL by its human receptors TACI and BCMA obtained by molecular dynamics simulations. Although most of the key interactions can be obtained from the existing experimental information, new described interactions between human APRIL and its receptors can contribute to a better design of APRIL inhibitors.

1. Introduction

APRIL, also named TRDL-1, TALL2 or TNFS13A, is a type II membrane protein that belongs to the tumour necrosis factor (TNF) family. Ligands and receptors of this family can modulate a variety of biological processes including apoptosis initialization, development of lymphoid organs and regulation of immune cells so APRIL is expressed by different cellular types, including immune cells like monocytes, macrophages, dendritic cells, neutrophils and T and B cells and others cells outside the immune system like epithelial cells, osteoclasts and tumour cells [1,2].

APRIL binds the receptors transmembrane activator and CAML interactor (TACI) and B cell maturation antigen (BCMA) that are members of the TNF receptors family (TNFRs) [2] and it can also interact with HSPGs (heparan sulphate proteoglycans), which are not related to the TNFRs [3,4]. BCMA has only one CRD (cysteine-rich domain) being structurally different from the TNFRs members that usually have several CRDs [5]. On the other hand, TACI has two CRD although only the second one is crucial for high affinity binding with APRIL. Both, BCMA and TACI have a conserved motif known as DxL that consists of six residues (Phe/Tyr/Trp)-Asp-X-Leu-(Val/Thr)-(Arg/Gly) and it is essential for the binding ligand–receptor [6] (Figs. S1 and S2). The binding of APRIL to HSPGs, involves interactions between acidic sulphated glycosaminoglycan (GAG) side chains of proteoglycans with two different binding sites in APRIL: the basic NH_2 terminal and basic residues located on the surface of the molecule opposite of the receptor binding pocket [4].

Since APRIL was discovered, it has been related to autoimmune diseases like systemic lupus erythematosus (SLE), rheumatoid arthritis (RA), Sjögren's syndrome (SS) and multiple sclerosis (MS). Murine models and patients with SLE present high levels of APRIL mRNA [7]. Inhibition of APRIL with TACI-Ig on mices with SLE results in the inhibition of symptoms and an increase of survival [8]. In the case of murine models with RA the inhibition of APRIL (also with TACI-Ig) results in a decrease of the inflammation and the significantly delay of the disease [9]. Moreover, in patients with SS and MS high levels of APRIL have been detected [7].

An important role of APRIL has been described in different types of tumour cell lines and in a variety of primary tumour tissues where, in contrast with the normal ones, high mRNA levels have been detected [1]. APRIL transgenic mice develop lymphoid tumours that resemble human chronic lymphocytic leukaemia (CLL) [10]. The analysis of CLL patients shows an increase in circulating APRIL levels that correlate with reduced overall patient survival. In CLL, APRIL stimulates the proliferation and survival of tumour cells and it might also protect them from apoptosis [11]. The effect of APRIL in promoting leukaemia is also observed in other B cell

* Corresponding author. Tel.: +34 93 4039263; fax: +34 93 4021231.
E-mail address: jaime.rubio@ub.edu (J. Rubio-Martinez).

1093-3263/$ – see front matter © 2012 Elsevier Inc. All rights reserved.
http://dx.doi.org/10.1016/j.jmgm.2012.11.002

malignancies and solid tumours like in non-Hodgkin's lymphomas (NHL) that encompass a large number of cancers that affects B cell and T cells [12–14].

APRIL is encoded by chromosome 17 in humans and chromosome 11 in mice, close to another TNF family member related with the apoptosis (TWEAK). The human APRIL gene contains six exons that combined by alternative splicing can generate three different mRNAs encoding the β, γ and δ forms of the protein. APRIL consists of a 28-amino acid cytoplasmatic domain, a 21-amino acid transmembrane domain and a 201-amino acid extracellular domain that includes the TNF domain. It forms a non covalent homotrimer and it is processed within the Golgi apparatus to a soluble form and it is thus normally secreted [2,15].

The design of new compounds that bind APRIL appears to be a promising way to treat cancer and autoimmune diseases. In order to better understand the main interactions between APRIL and its receptors, we report the results of molecular dynamics simulations of murine and human APRIL bound to human TACI and BCMA. Here new interactions are described that with those described experimentally can contribute to a better design of APRIL inhibitors.

2. Computational details

All the calculations described in the present work were carried out at molecular mechanics level using Amber ff99SB force field [16] with AMBER v.11 suite of program [17]. All simulations were carried out under periodic boundary conditions where long-range electrostatics interactions were treated by using the particle-mesh-Ewald method [18] and the cutoff distance was kept to 9 Å to compute the non bonded interactions. The solvent was considered explicitly using TIP3P water molecules [19].

The ptraj and MMPBSA.py [20] modules of AMBER v.11 package were used to identify intermolecular hydrogen bonds, van der Waals and electrostatic interactions, to obtain total binding free energies and to analyse the contribution of each receptor residue to the total binding free energy for all the studied complexes during the production time. All figures were done with the VMD graphics program [21].

2.1. Construction of APRIL–receptor complexes

The initial 3D structures of the complexes murine APRIL with human TACI (mAPRIL–TACI) and murine APRIL with human BCMA (mAPRIL–BCMA) were taken from the Protein Data Bank (http://www.rcsb.org/pdb) with access codes 1XU1 and 1XU2 respectively [22]. The complexes are formed by a trimeric murine APRIL, that contains only the extracellular domain of the protein (residues 105–241) and three units of a shorted human TACI (TACI_d2, residues 71–109) for the first complex and three units of a human BCMA (residues 8–42) for the second complex. Since human and murine APRIL share 85% sequence identity in the TNF domain (Fig. S3), the hAPRIL–TACI and hAPRIL–BCMA complexes were constructed by homology modelling using the 3D structure of mAPRIL–receptor complexes as templates. Side chain coordinates of non-identical residues were generated using the leap module of AMBER v.11 software. We assumed that they exhibit the same fold as those containing murine APRIL. Finally, TIP3P water molecules and counterions were added to the system.

2.2. Energy minimizations

All complexes were energy minimized to remove possible steric stress by the same multi-step procedure in order to ensure minimum structural changes from the initial templates. First, only hydrogen positions were optimized. Second water molecules, ions and terminal atoms of the complexes were allowed to relax while the rest of the system was kept frozen. Third, side chains of APRIL and the corresponding receptor were relaxed as well as water molecules. Fourth, all main chain atoms of the receptor were relaxed, and finally all atoms were allowed to move. We used the steepest descent method followed by the conjugated gradient method. The final RMS gradient, achieved with 50,000 iterations, was 0.01 kcal/(mol Å), which is a reasonable gradient for a local minimum.

2.3. Molecular dynamics simulations

Molecular dynamics (MD) simulation for the different complexes was performed at a constant temperature of 300 K by coupling the system to a thermal bath using Berendsen's [23] algorithm as implemented in AMBER v.11, with a time coupling constant of 0.2 ps. Time step was set to 2 fs and bond lengths involving hydrogen atoms were constrained to equilibrium lengths using the SHAKE algorithm [24]. A cut-off of 9 Å for non-bonded interactions was used. MD simulation began by heating the minimized structures to 300 K over a period of 100 ps at a constant rate of 30 K/10 ps. The second step of 100 ps was done in the NPT ensemble (1 atm, 300 K), to increase the density of the system, using a weak-coupling algorithm analogous to temperature coupling [23], as implemented in AMBER v.11. Finally, 40 ns of MD calculation was performed at a constant temperature of 300 K in the canonical ensemble (NVT).

2.4. Free energy calculations

Binding free energies were calculated using the molecular mechanics generalized Born surface area (MMGBSA) and the molecular mechanics Poisson–Boltzmann surface area (MMPBSA) algorithms implemented in the AMBER v.11 package [20]. The total binding free energy can be calculated accordingly to the equation:

$$\Delta G_{\text{binding}} = \Delta G^{\text{gas}} + \Delta G^{\text{solv}} - T\,\Delta S$$

where ΔG^{gas} is the gas phase interaction energy which is the sum of the internal energy and the noncovalent van der Waals (ΔG_{vdW}) and electrostatic (ΔG_{elec}) molecular mechanics energies. ΔG^{solv} is obtained by summing the polar (ΔG_{polar}) and nonpolar ($\Delta G_{\text{nonpolar}}$) terms. ΔG_{polar} can be calculated solving the Poisson–Boltzmann (PB) equation or by the generalized Born (GB) method. For the GB method we used the Onufriev approximation [25] as implemented in the AMBER v.11 package (igb = 5). $\Delta G_{\text{nonpolar}}$ is calculated using the equation $\Delta G_{\text{nonpolar}} = \gamma\ \text{SASA} + \beta$, where SASA is the solvent-accessible surface area. ΔS is the entropic term.

Calculations were carried out with the parameters: (1) values for interior and exterior dielectric constants of 1 and 80 respectively. (2) The MMPBSA.py default values for γ and β constants (0.00542 kcal/(mol Å^2) and −1.008 kcal/mol in MMPBSA and 0.0072 kcal/(mol Å^2) and 0 kcal/mol in MMGBSA, respectively).

Binding free energies for the complexes were calculated for the whole MD, with MMPBSA and MMGBSA algorithms described before, using 100 snapshots for each ns of MD. The contribution of each BCMA and TACI residues to the total binding free energy of the complexes was analysed using the MMGBSA decomposition protocol as implemented in AMBER v.11. All energy components were calculated using 500 snapshots corresponding to the last 5 ns of the molecular dynamic. Changes in entropy were ignored.

2.5. Analysis of the hydrogen bonds

The hydrogen bonds between both receptors and APRIL were characterized using the *ptraj* module of AMBER v.11 and over the

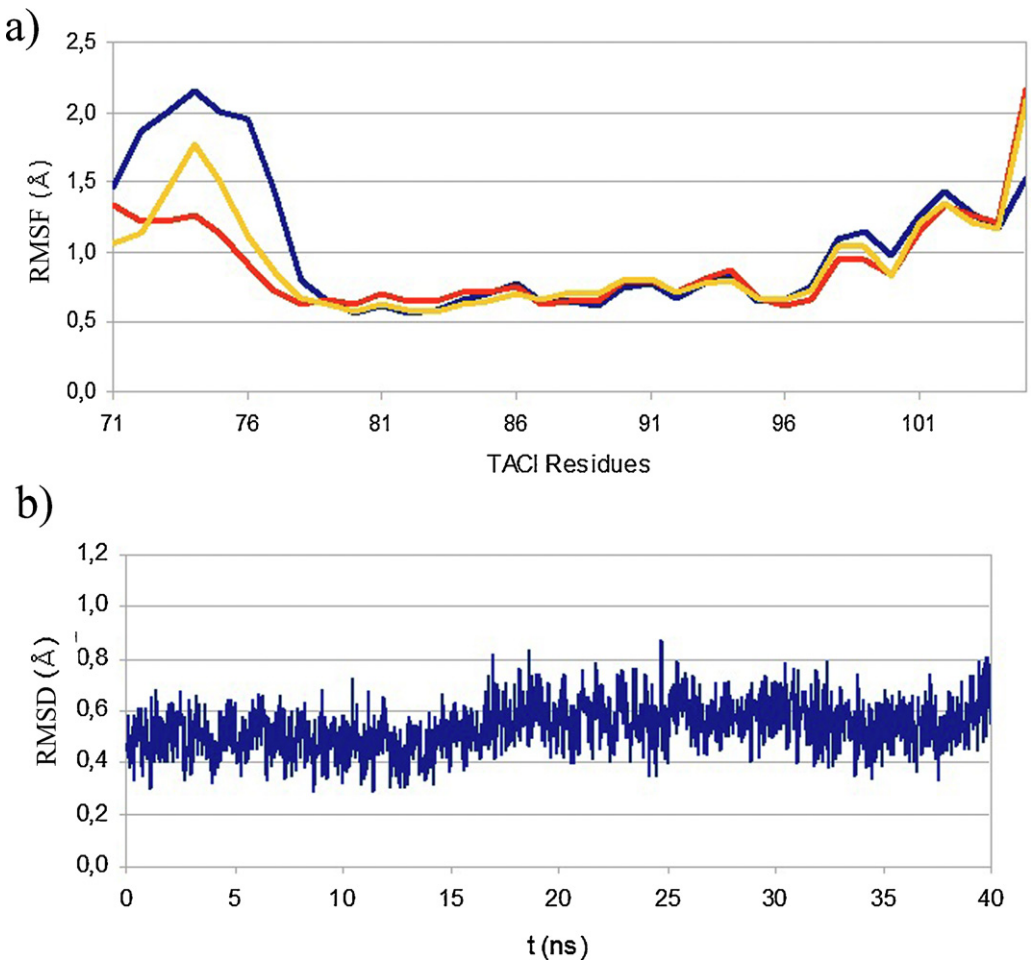

Fig. 1. (a) Atomic positional fluctuations (RMSF) by residue for each TACI chain (blue, green and red) in the hAPRIL–TACI complex. Residues with more than 0.7 Å of fluctuation were removed for the posterior RMSD analysis. (b) RMSD of TACI along the molecular dynamics. (For interpretation of the references to colour in this figure legend, the reader is referred to the web version of the article.)

last 5 ns of simulation time. Parameters used for hydrogen bonding were: (1) hydrogen acceptor–donor atom distances of less than 3.5 Å and (2) acceptor–H-donor angles (Θ_{HB}) of more than 120°. The percentage of structures in which the hydrogen bond satisfies the conditions of distance and angle is quantified by percentage of occupation. Values for the hydrogen bond angles are reported as $180 - \Theta_{HB}$, as are calculated in AMBER v.11.

3. Results and discussion

3.1. Structural analysis

The quality of the modelled structures was assessed using the program PROCHECK [26], which reported that 99.5% and 99.1% of the residues fell within the allowed regions of the Ramachandran plot for hAPRIL–TACI and hAPRIL–BCMA complexes, respectively.

In order to locate the flexible regions of the human complexes (hAPRIL–TACI and hAPRIL–BCMA), we analysed the atomic positional fluctuations (RMSF) for each residue of the complexes along the molecular dynamic simulations. For this purpose the RMSF was performed with *ptraj* module of Amber v.11, being superposed the APRIL (Figs. S4a and S5a) or the receptors (Figs. 1a and 2a) of each complex.From the RMSF analysis, we detected those regions with more changes along the molecular dynamics. As it can be seen, the major part of APRIL residues show small fluctuations except in the big loop around the residue 190. With respect to the receptors, it can be seen that TACI makes some fluctuations in the terminal residues, a behaviour that is less pronounced in the BCMA receptor. Residues with more than 0.7 Å of fluctuation were removed for the posterior RMSD analysis. Thus, we performed a root mean square deviation (RMSD) calculation with *ptraj* module for human complexes to have an overall view of the changes of the complexes without those loops with high fluctuations.

The RMSD calculation was performed for: (1) the APRIL of each complex (Figs. S4b and S5b) and (2) the receptors (TACI and BCMA) of each complex (Figs. 1b and 2b). It is important to note that, after removing flexible loops, all the analysed systems present a very good behaviour of their respective RMSD values.

3.2. Energetic analysis

The evolution of $\Delta G_{binding}$ for murine and human–APRIL complexes versus time throughout their molecular dynamics trajectories is shown in Fig. S6. We can see that all the complexes are stabilized although the human complexes have more fluctuations that the murine complexes. However the analysis of atomic interactions in all the complexes was made over the last 5 ns of the molecular dynamics. The entropic contribution to the binding energy has been neglected because our goal is not to reproduce the absolute binding energies but to quantify and analyse the interactions changes between APRIL and its receptors.

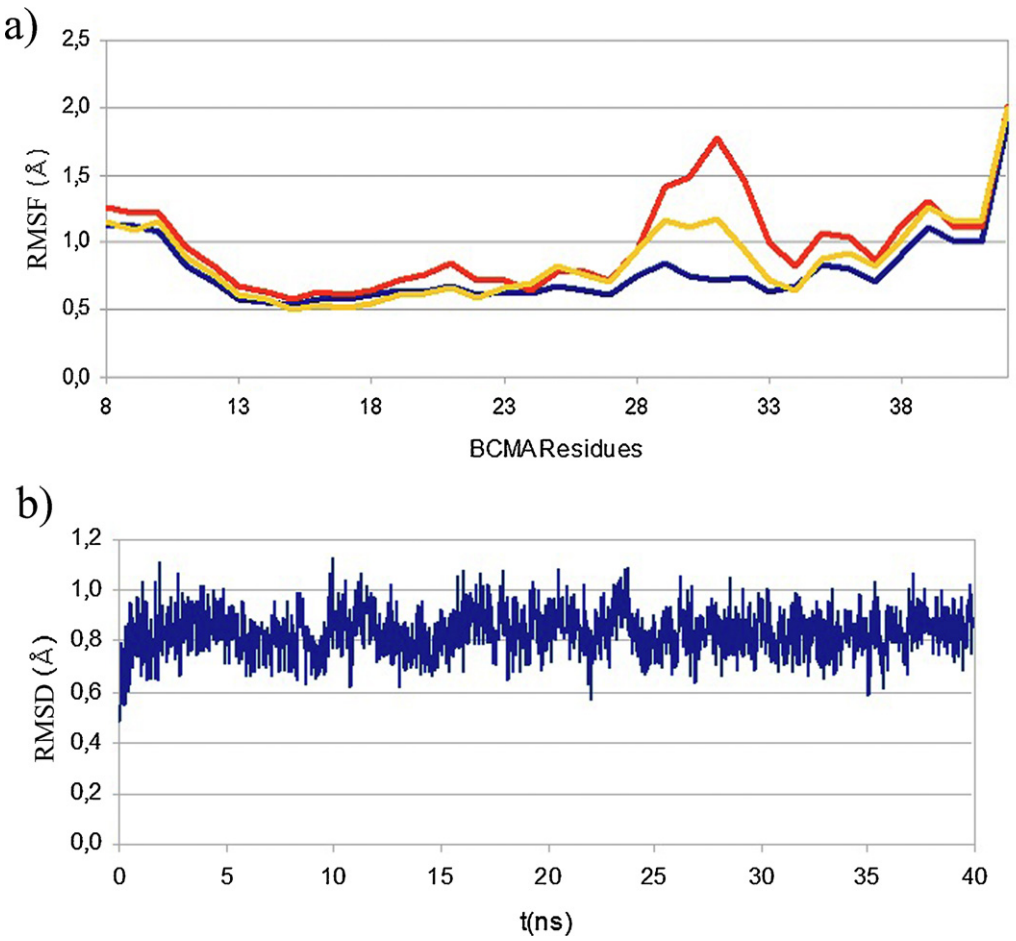

Fig. 2. (a) Atomic positional fluctuations (RMSF) by residue for each BCMA chain (blue, green and red) in the hAPRIL–BCMA complex. Residues with more than 0.7 Å of fluctuation were removed for the posterior RMSD analysis. (b) RMSD of BCMA along the molecular dynamics. (For interpretation of the references to colour in this figure legend, the reader is referred to the web version of the article.)

3.3. *mAPRIL–TACI complex*

In Table 1 we list the relevant data for hydrogen bonds that we have found along the last 5 ns of the molecular dynamic. The residue Asp^{80}, which belongs to the DxL motif (Fig. 3 and Fig. S1), uses its two side chain carbonyl oxygens atoms to form hydrogen bonds with the hydrogens atoms of the guanidinium moiety of the mAPRIL, Arg^{222}. It is important to note that this interaction, as others interactions shown in this work, is a dynamic bond. That is, the involved atoms are different at different times but they belong to the same residues. The percentage of occupation is close to 100% because all atoms involved have a good distance and angle to form the hydrogen bond. Gln^{95} that is positioned at the h1h2 loop (Fig. 3) forms hydrogen bond with Arg^{197} from chain A and Val^{165}, Met^{191} and Phe^{167} from chain B of APRIL. The percentage for these hydrogen bonds is almost 100%. Hymowitz et al. [22] suggested that this network can contribute to stabilize the conformation of different parts of APRIL that are not well ordered without the receptor. However, experimental information does not attribute an important contribution to this residue. A possible explanation would be that only the hydrogen bond formed by the carbonyl of Gln^{95}, would be capable to induce the necessary changes in APRIL. On the other hand, Gln^{95} does not have an equivalent residue in the BCMA receptor. Therefore, it seems probable that this loop has an important role in the selectivity of TACI versus APRIL. The only hydrogen bonds described in the X-ray reference [22] are those formed by Asp^{80} and Gln^{95}. However, after the MD, other hydrogen bonds have been

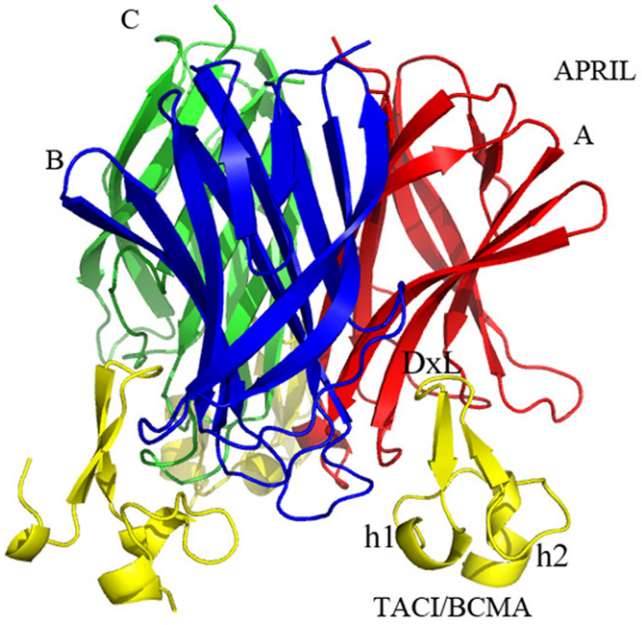

Fig. 3. Ribbon structure for mAPRIL/TACI. APRIL trimer is shown in blue, red and green and TACI is shown in yellow. (For interpretation of the references to colour in this figure legend, the reader is referred to the web version of the article.)

Table 1
Hydrogen bonds formed between murine APRIL and human TACI over the last 5 ns of the molecular dynamics.

TACI	mAPRIL	Distance/Å	RMSD/Å	Angle/°	RMSD/°	% occupation
ASP^{80} OD1	ARG^{222}B HH12	2.94	0.17	38.5	13.0	93.6
	ARG^{222}B HH22	2.88	0.20	33.0	11.5	84.8
ASP^{80} OD2	ARG^{222}B HH12	2.95	0.18	32.5	13.7	94.4
	ARG^{222}B HH22	3.09	0.24	40.0	12.8	77.2
LEU^{82} O	ARG^{186}B HH11	2.86	0.13	25.8	9.8	100.0
LEU^{83} O	ARG^{186}B HH12	3.12	0.21	42.5	10.0	55.2
SER^{91} O	ARG^{197}A HH12	2.86	0.15	26.4	12.8	99.2
	ARG^{197}A HH22	3.09	0.22	41.9	10.6	47.6
SER^{91} HG	ASP^{196}A OD1	2.73	0.17	20.7	11.1	37.6
	ASP^{196}A OD1	2.79	0.26	23.4	15.4	38.0
GLN^{95} O	PHE^{167}B H	2.98	0.15	15.4	7.4	99.2
GLN^{95} HE21	MET^{191}B O	2.88	0.14	23.8	11.1	100.0
GLN^{95} HE22	VAL^{165}B O	2.87	0.14	22.5	10.6	99.6
GLN^{95} OE1	ARG^{197}A HH21	2.87	0.16	27.0	11.7	98.0
	ARG^{197}A HE	3.05	0.20	34.1	10.2	83.6

found. Thus, residue Ser^{91} from h1, forms a dynamic hydrogen bond where its main carbonyl oxygen and the hydrogen from its side chain interacts with side chain hydrogen atoms of Arg^{197} and with the carbonyl oxygen of Asp^{196}. The percentages of occupation are close to 100% and 60% respectively. In the second case, this indicates that the hydrogen bond is not stable along all the last 5 ns of the molecular dynamic. Finally both leucines from DxL motif, Leu^{82} and Leu^{83}, interact with Arg^{186} with a great percentage of occupation of 100% for the first one and a modest 55.2% for the second one. These leucines are clearly important for the binding of APRIL to its receptors. This fact clearly appears in the mutational analysis study performed by Hymowitz et al. [22] although hydrogen bonds for these two residues were not described.

The values of ΔG_{vdW} during the production time of each residue of TACI are shown in Fig. S7a. Two regions, where the most important contribution to the binding come from the van der Waals interaction, are clearly defined, one in the DxL motif and another one in the h1h2 loop. His^{81}, Leu^{82}, Leu^{83} and Arg^{84} form the first one, being the two leucines residues the most important. The second zone includes residues from Gln^{95} to Gln^{99}. Residue Gln^{95}, has the biggest contribution, reaffirming it importance. Since Pro^{97} only has a modest van der Waals contribution to APRIL binding but seems to be important from an experimental point of view [21], we suggest also an indirect role in the binding of TACI to mAPRIL, contributing to the structural stability. In addition, Lys^{98} has also a modest van der Waals contribution to APRIL binding. However in this case, experimental results are in agreement with our results and neither direct nor indirect role in APRIL binding has been attributed to this residue. Finally, residues Ile^{87} and Ile^{92}, located between these two zones, present important van der Waals contributions and have a notable effect on APRIL binding. Both residues have been shown to be important experimentally [22].

The ΔG_{elec} energies calculated along the molecular dynamic simulation are shown in Fig. S7b. As expected, only charged residues have a remarkable electrostatic contribution to the binding. Asp^{80} and Asp^{85} are the most important residues. Asp^{80}, as was explained before, showed a stable hydrogen bond. Its importance is clearly justified by experimental results [22]. The Asp^{85} residue has an important electrostatic contribution to the binding; however is cancelled due to the solvation effect. Also, Arg^{84} shows an important positive electrostatic contribution to the binding, but this contribution is approximately compensated by its van der Waals contribution. Some other residues in the N-terminal have positive electrostatic interaction but experimentally this region has been detected as one with a high conformation heterogeneity and lack of restraints.

Finally, we analysed the total $\Delta G_{binding}$ results shown in Fig. 4a. Three residues located in the DxL region Asp^{80}, Leu^{82} and Leu^{83} and residues Ile^{87} and Ile^{92} have an important energy contribution to the binding in concordance with the previous results. The residue Gln^{95} that has a great energetic contribution has been described experimentally to form different hydrogen bonds. The last residue found that has an important energy contribution is the Ser^{91}. This serine appears to form hydrogen bonds with the Arg^{197} and Asp^{196} residues of mAPRIL. On the other hand Asp^{85}, with an important electrostatic contribution to the binding, does not have an important contribution to the total binding energy due to the

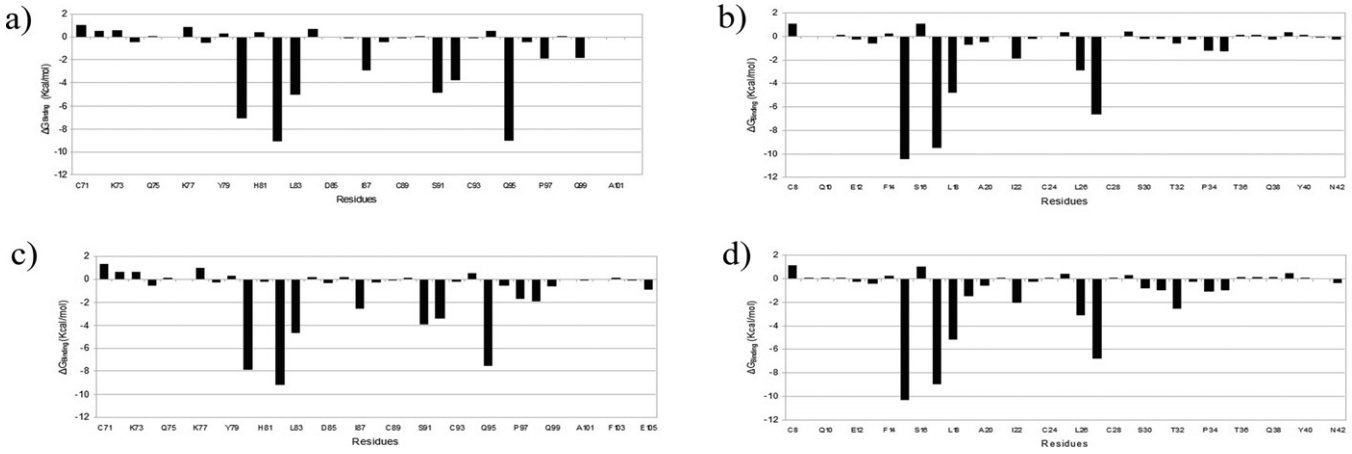

Fig. 4. $\Delta G_{binding}$ contribution to the total binding free energy of each residue of TACI and BCMA for the complexes in the last 5 ns of the molecular dynamics. (a) mAPRIL–TACI, (b) mAPRIL–BCMA, (c) hAPRIL–TACI and (d) hAPRIL–BCMA.

Table 2
Hydrogen bonds formed between murine APRIL and human BCMA over the last 5 ns of the molecular dynamics.

BCMA	mAPRIL	Distance/Å	RMSD/Å	Angle/°	RMSD/°	% occupation
ASP^{15} OD1	ARG^{222}B HH12	2.94	0.17	32.4	12.8	96.8
	ARG^{222}B HH22	3.16	0.16	45.9	8.7	78.8
ASP^{15} OD2	ARG^{222}B HH22	2.82	0.12	32.0	10.5	99.2
	ARG^{222}B HH12	2.95	0.16	44.0	9.4	90.0
LEU^{17} O	ARG^{186}B HH21	2.85	0.12	20.9	10.6	99.6
	ARG^{186}B HE	3.14	0.20	36.8	8.9	57.2
ARG^{27} HH12	ASP^{123}B OD2	2.78	0.10	19.3	9.2	100.0
ARG^{27} HH22	ASP^{123}B OD1	2.83	0.14	24.7	11.3	99.6
	ASP^{123}B OD2	3.09	0.21	40.0	8.2	91.2

unfavourable contribution of the solvation energy, in agreement with the experimental results [22].

Finally, it is important to note that residues Phe^{78}, Tyr^{79}, Gly^{94} and His^{96} are relevant from an experimental point of view but it has been suggested a structural role. Our results confirm this fact and these residues do not have important interactions with APRIL, so intra-ligand interactions should give importance to these residues. Our results support the experimental ones [22].

3.4. mAPRIL–BCMA complex

For the mAPRIL–BCMA complex we found three main hydrogen bonds which are listed in Table 2. These hydrogen bonds have a great percentage of occupation and have optimum geometrical hydrogen bonds parameters. Asp^{15} is located in the DxL motif and its carbonyl group oxygens interacts with the hydrogen atoms of the guanidinium moiety of Arg^{222} of APRIL chain's B. This hydrogen bond is equivalent to that formed by Asp^{80} and Arg^{222} in mAPRIL–TACI indicating the importance of this interaction. A second hydrogen bond, formed by Leu^{17} of the DxL motif and Arg^{186} of mAPRIL, has also been found in the mAPRIL–TACI complex, although it has not been found experimentally. Finally, Arg^{27} makes a hydrogen bond with the carbonyl oxygen of Asp^{123} of mAPRIL. Our results represent a theoretical confirmation of the suggestion made by Wallweber et al. [27] by comparison with BCMA–BAFF complex. It is important to note that experimental site-directed mutagenesis analysis shows that these residues are important for APRIL binding and that when replacing Arg^{27} by alanine there is an important loss in the APRIL binding affinity but with an important gain in BAFF binding affinity [27].

In Fig. S8a, we show the ΔG_{vdW} contribution for each residue of BCMA during the production time to the protein–protein interactions. As in the case of TACI, two important hydrophobic regions are clearly defined, one in the DxL motif and another one in the equivalent counterpart of the h1h2 loop of TACI. Residues Leu^{17} and Leu^{18}, that form part of the DxL motif, are the most important. Outside the DxL motif, the most important van der Waals interaction corresponds to Leu^{26} that has in Ile^{92} its equivalent residue in TACI. Adjacent residues, Arg^{27}, Ser^{30}, Asn^{31} and Thr^{32} form a compact hydrophobic region. Ile^{22} shows a noticeable contribution to the binding. A shotgun alanine scan of the single extracellular CRD of BCMA shows that the single mutation of Ile^{22} by a lysine produced a modified BCMA with great selectivity over APRIL in front of BAFF [27]. Tyr^{13}, outside the DxL motif, presents a little but appreciable van der Waals interaction with APRIL. It has been suggested previously [27] that a possible hydrogen bond with Asp^{15} and Arg^{27} may be necessary to place adequately Asp^{15} to interact with Arg^{222}. By analysing the hydrogen bonds we confirm this hypothesis because we found that Tyr^{13} makes a hydrogen bond with the oxygen of both Asp^{15} and Arg^{27} with a percentage of occupation of 100% and 82%, respectively. However, the effect of a mutation in this residue is important on APRIL binding but has no effect on BAFF binding.

As it can be seen in Fig. S8b, only two residues of BCMA, Asp^{15} and Glu^{12}, have a great electrostatic contribution to the APRIL binding.

Finally, the $\Delta G_{binding}$ (Fig. 4b) shows the total contribution of each BCMA residue to APRIL binding. The Asp^{15}, Leu^{17} and Leu^{18} from DxL motif have the greatest energy of interaction. Arg^{27} also shows a great energy and it fits with our previous results in which Arg^{27} makes a hydrogen bond with Asp^{123} of APRIL. The last residue that it is important to the binding is Leu^{26} that has the same function that Ile^{92} in TACI shows a modest energy contribution.

3.5. hAPRIL–TACI complex

In Table 3 we show the relevant data for the hydrogen bonds that we have found. Two of them have been detected in the experimental studies of mAPRIL–TACI and also in our computational

Table 3
Hydrogen bonds formed between human APRIL and human TACI over the last 5 ns of the molecular dynamics.

TACI	hAPRIL	Distance/Å	RMSD/Å	Angle/°	RMSD/°	% occupation
ASP^{80} OD1	ARG^{231}B HH11	2.97	0.18	35.7	12.9	96.0
	ARG^{231}B HH22	3.03	0.21	35.9	13.2	88.4
ASP^{80} OD2	ARG^{231}B HH22	2.96	0.24	37.4	13.4	76.4
	ARG^{231}B HH11	2.91	0.18	36.4	13.2	96.8
LEU^{82} O	ARG^{195}B HH12	2.88	0.12	22.0	8.8	98.8
LEU^{83} O	ARG^{195}B HH11	3.01	0.21	43.3	9.3	67.6
ARG^{84} HH22	THR^{192}B OG1	3.00	0.18	30.4	13.7	64.4
ARG^{84} HH12		3.05	0.20	32.9	13.2	60.0
ASP^{85} OD2	TYR^{208}A HH	2.74	0.16	15.6	8.6	71.2
SER^{91} O	ARG^{206}A HH21	3.05	0.21	41.1	11.1	70.8
	ARG^{206}A HE	2.94	0.18	29.1	13.4	89.2
SER^{91} HG	ASP^{205}A OD2	2.76	0.21	19.8	11.1	38.8
	ASP^{205}A OD1	2.70	0.16	17.2	9.8	48.0
GLN^{95} O	PHE^{176}B H	2.99	0.15	13.9	7.6	99.2
GLN^{95} OE1	ARG^{206}A HH11	2.85	0.13	13.9	7.6	99.2
GLN^{95} HE21	MET^{200}B O	2.89	0.14	27.0	11.5	100.0
GLN^{95} HE22	VAL^{174}B O	2.83	0.11	17.6	9.4	100.0

Table 4
Hydrogen bonds formed between human APRIL and human BCMA over the last 5 ns of the molecular dynamics.

BCMA	hAPRIL	Distance/Å	RMSD/Å	Angle/°	RMSD/°	% occupation
ASP^{15} OD1	ARG^{231}B HH22	2.84	0.13	32.9	10.6	97.6
	ARG^{231}B HH11	2.98	0.19	45.5	9.3	83.2
ASP^{15} OD2	ARG^{231}B HH11	2.89	0.15	28.1	11.8	98.8
	ARG^{231}B HH22	3.19	0.17	45.7	8.2	80.4
LEU^{17} O	ARG^{195}B HH12	2.88	0.12	24.1	9.7	99.6
LEU^{18} O	ARG^{195}B HH11	3.16	0.21	37.4	11.1	43.6
ARG^{27} HH22	ASP^{132}B OD1	2.83	0.12	19.1	9.6	100.0
	ASP^{132}B OD2	3.17	0.20	43.0	6.9	71.6
ARG^{27} HH12	ASP^{132}B OD2	2.75	0.08	16.9	8.6	100.0
THR^{32} OG1	ARG^{233}B HE	2.96	0.16	28.5	12.5	41.6

study. These two hydrogen bonds involve Asp^{80} and Gln^{95} residues and were described previously. Asp^{80} interacts with Arg^{231} residue and Gln^{95} interacts with different residues from hAPRIL forming a complex network as in the murine complex. In this complex, the percentages of occupation of these hydrogen bonds are also close to 100%. As we mentioned previously this interaction network can stabilize the conformation of APRIL. As in the mAPRIL–TACI complex, here it is shown that both leucines, Leu^{82} and Leu^{83}, from the DxL motif make hydrogen bonds with Arg^{195} from monomer B of APRIL (equivalent to the residue Arg^{186} in the mAPRIL). Leu^{83} has a modest 67.6% of occupation. Arg^{84} makes a hydrogen bond with Thr^{192} from monomer B of APRIL. Experimentally, this Arg^{84} has been shown to be important to BAFF binding but not to APRIL binding trough mutational analysis. This bond does not appear in the mAPRIL–TACI although an equivalent residue exists (Thr^{183}). The hydrogen bond formed by one of the side chain carbonyl group oxygen of Asp^{85} with one of the hydrogen of Tyr^{208} has a modest occupation of 71.2%. This is because the bond is lost during part of the production time. Asp^{205} of APRIL used its chain carbonyl group oxygen to bind to Ser^{91} of TACI. Like in the Asp^{85} case, both bonds alone have a modest occupation but now Asp^{205} has a great occupation during the production time, making important this APRIL residue. This serine residue also interacts with Arg^{206} and its interactions are also presents in mAPRIL–TACI (Asp^{196} and Arg^{197}).

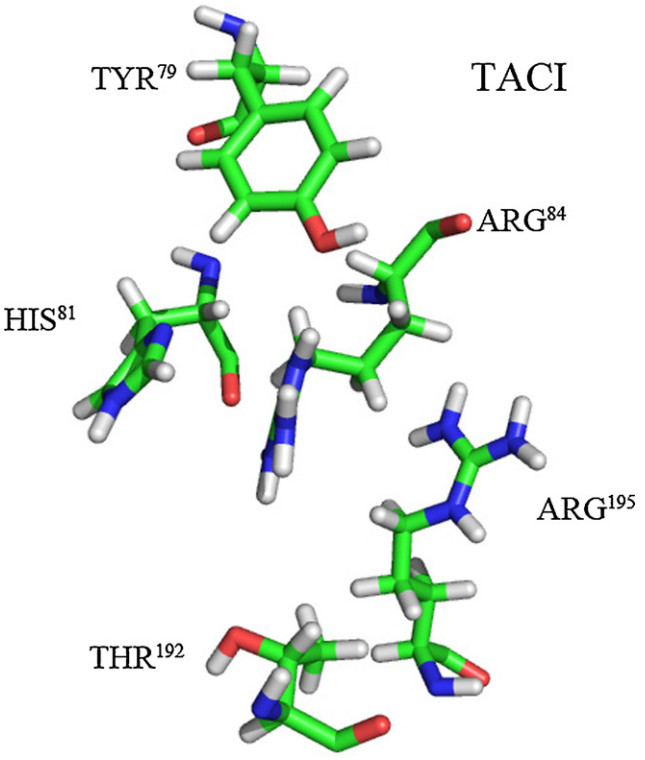

Fig. 5. Spatial representation of the DxL mutated residues of TACI with respect to BCMA. Arg^{195} and Thr^{192} are APRIL residues.

The ΔG_{vdW} and ΔG_{elec} energy contributions of each residue for the production time are shown in Fig. S9. The $\Delta G_{binding}$ is shown in Fig. 4c. It is worth to note that, hydrogen bonds coming from Arg^{84} and Asp^{85}, that are not presents in the murine system, do not have contribution to the total binding energy due to the solvation effect and to electrostatic and van der Waals cancellations. As a consequence, these graphics have the same profile than those obtained for mAPRIL–TACI with little differences in the energy values. These results demonstrate that differences on the structure of mAPRIL and APRIL do not interfere with the binding to TACI being the residues involved the same.

In order to confirm if the results for the important residues obtained in the last 5 ns of the molecular dynamic are correct we also perform the analysis for several time intervals of the simulation. These results are shown in Fig. S11, where we can see the same profile for all the studied intervals along the simulation.

Finally, an important point to be discussed concerns the ionization state of the residues located at the DxL motif, in particular the His^{81} residue that could be protonated. However, if we analyse this His^{81} residue (see Fig. 5) in the production period, it can be seen that Arg^{84}, also in the DxL motif, is close to it. Thus, the protonation of His^{81} will be unfavourable. However, more quantitative analysis should be done to completely rule out the possibility of a protonated histidine.

3.6. hAPRIL–BCMA complex

Relevant data of the hydrogen bonds that we have found along the production time for the hAPRIL–BCMA complex is shown in Table 4. Clearly, three BCMA residues, Asp^{15}, Leu^{17} and Arg^{27} were also present in mAPRIL–BCMA complex analysed previously. Asp^{15} formed a dynamic hydrogen bond with Arg^{231} of monomer B of APRIL and it has a great percentage of occupation. Arg^{27} also formed a dynamic hydrogen bond with Asp^{132} of monomer B having a percentage of occupation close to 100%. Finally, Leu^{17} interacts with Arg^{195} which also interacts with Leu^{18} with a modest percentage of occupation (43.6%).

In Fig. S10 we show the ΔG_{vdW} and ΔG_{elec} energy contribution of each residue of BCMA along the last 5 ns of the molecular dynamics. $\Delta G_{binding}$ energy contribution is shown in Fig. 4d. As in the case of hAPRIL–TACI, the results of hAPRIL–BCMA are practically the same as those obtained for mAPRIL–BCMA. The profiles of ΔG_{elec} and ΔG_{vdw} only differed slightly on the energy values. The $\Delta G_{binding}$ has some little differences between residue Ser^{30} and Thr^{32} but the important residues are present in both graphics. These results show that there are not important differences between mAPRIL–BCMA and hAPRIL–BCMA complexes when it refers to the residues for binding to APRIL.

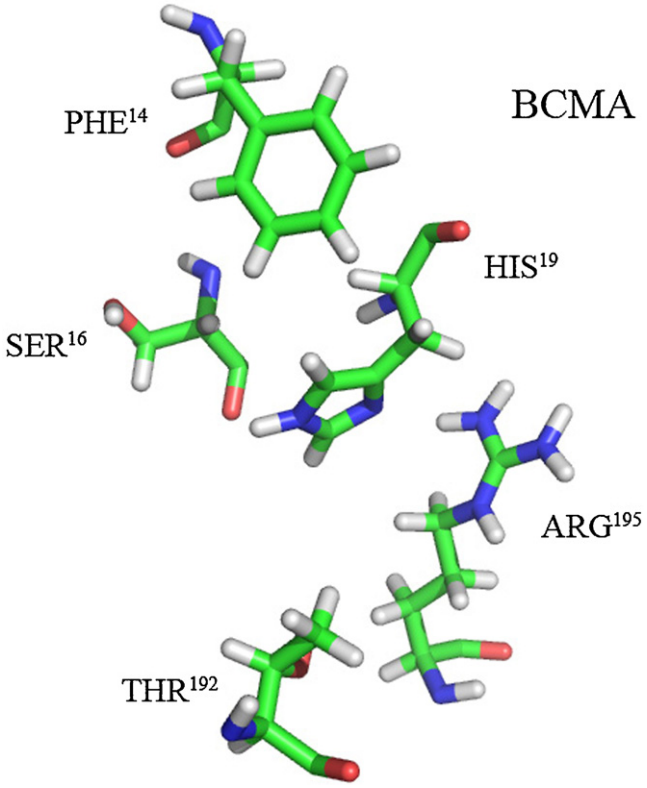

Fig. 6. Spatial representation of the DxL mutated residues of BCMA with respect to TACI. Arg^{195} and Thr^{192} are APRIL residues.

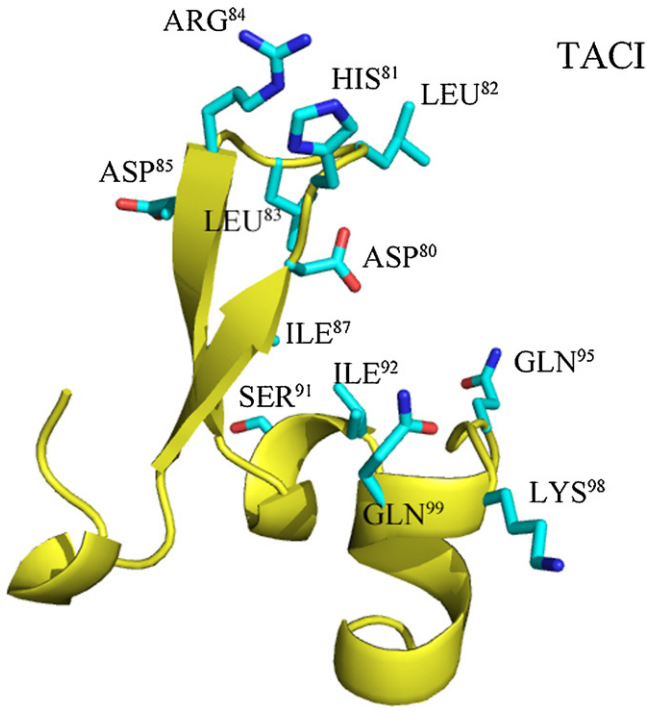

Fig. 7. Spatial representation of the important TACI residues to bind APRIL.

Finally, as in the previous system, we can discuss the ionization state of the residues located at the DxL motif. There are three mutated residues, with respect to the TACI receptor, and one of them, the His^{19}, could be protonated. However, the presence of Arg^{195} (see Fig. 6) from APRIL makes this protonation unfavourable. It is worth to note that the Arg^{195} is also near the Arg^{84} from TACI, but the different length of the side chains of Arg^{84} with respect to His^{19} make possible the coexistence of both arginines despite their positive charge. However, as in the previous case, a more quantitative analysis should be done to completely rule out the possibility of a protonated histidine.

3.7. Pairwise analysis

The results for the pairwise analysis for mAPRIL–TACI and hAPRIL–TACI are shown in Tables S1 and S2. In both complexes, there are a lot of interactions in common, like those interactions of Asp^{80}, His^{81}, Leu^{82}, Leu^{83}, Ile^{87}, Ile^{92}, Gln^{95} and Gln^{99}. With respect to the Arg^{84} in the murine complex, it loses the interaction with Arg^{186} (Arg^{195} in hAPRIL). However Ser^{91} gains an interaction with Asp^{194} that in the hAPRIL is substituted by His^{203}. Also Lys^{98} makes two more interactions with Asp^{121} and Asp^{123} (Asp^{130} and Asp^{132} in hAPRIL). In the human complex it has been detected the interaction between Asp^{85} and Tyr^{208} that does not appear in the murine complex despite it has the Tyr^{199}. Also in the murine complex there exists the interaction between Ser^{88} and Asp^{196} that does not appear in the human complex despite it has the Asp^{205}.

For the complexes of mAPRIL–BCMA and hAPRIL–BCMA the results of the pairwise analysis are shown in Tables S3 and S4. In both complexes, residues Asp^{15}, Leu^{17}, His^{19}, Leu^{26} and Arg^{27} make the same interactions with the same residues of APRIL. However, there are some differences in the comparative analysis between hAPRIL–BCMA and mAPRIL–BCMA. Thus, as regards to Leu^{18} and Thr^{32}, in the murine complex, it has not been detected the hydrogen bond with Arg^{186} (Arg^{195} in hAPRIL) and Asn^{224} (Arg^{233} in hAPRIL) respectively. Also in the human complex it has been identified the interactions between Ile^{22} and Asp^{205} and between Ser^{30} and Thr^{175}. However, despite equivalent residues exist in the murine complex (Asp^{196} and Thr^{166}), these interactions have not been detected.

In the comparison between the human complexes of APRIL with TACI and BCMA, we can see that in the DxL motif there are only small differences and that they come from the residues that are different in both receptors. TACI has interactions between His^{81} and Asp^{85} with Pro^{230} and Tyr^{208} of APRIL and these two residues are mutated to Ser^{16} and Ala^{20} in the BCMA receptor. Also in the DxL motif, residues His^{19} of BCMA and Arg^{84} of TACI have different contribution to the binding. The Arg^{84} of TACI makes a hydrogen bond with Thr^{192} and also interacts with His^{241} and Arg^{195} while His^{19} of BCMA only has van der Waals interaction with Arg^{195}. Out of the DxL the differences are more significant. Figs. 7 and 8 show the spatial representation of the residues that are important for the binding TACI and BCMA to human APRIL.

3.8. Pharmacophoric hypothesis

In first and second row of Table 5, we show those residues of TACI that have been detected as important for binding to APRIL and BAFF in shotgun alanine scanning experiments [27]. As it is usual in protein–protein interactions, contact surface between APRIL and its receptor is large and has different hotspots, making difficult to mimic all the existing interactions by a small molecule.

The fact that proteins are constituted by a great number of amino acid residues permits protein–protein interactions to be distributed along a large contact surface. To place adequately these interactions, proteins used amino acid residues that are important only from a structural point of view but they do not make any direct interaction. However, when trying to mimic these interactions by small molecules, those residues having only a structural role are not necessary because an adequate scaffold substitutes them. For this reason, those residues of TACI involved only in internal

Table 5
Summary of important residues of TACI and BCMA.

TACI-APRIL[a]	F78	Y79	D80	L82	L83			I87		I92	G94	Q95	H96	P97
TACI-BAFF[b]		Y79	D80	L82	L83	R84		I87			G94	Q95	H96	P97
STRUC[c]		Y79									G94		H96	
TACI-APRIL phar[d]			D80	L82	L83	R84	D85	I87						
BCMA-APRIL phar[e]			D15	L17	L18			I22	L26	R27				

[a] Residues important for binding TACI to APRIL from Ref. [22].
[b] Important residues for binding TACI to BAFF from Ref. [22].
[c] Residues only important for structural stability of TACI.
[d] Suggested residues for a pharmacophoric hypothesis of TACI–APRIL interactions.
[e] Suggested residues for a pharmacophoric hypothesis of BCMA–APRIL interactions. Residues in red are important for binding, residues in green are supposed to have a structural role and residues in blue have small contribution to the binding.

interaction or that contribute only to maintain their structures, have not been taken into account to generate the pharmacophoric hypothesis. Third row of Table 5 shows those residues we consider, taking into account the previous discussion, that do not make direct interactions with APRIL. Thus, fourth row of Table 5 shows the final suggested interaction points. Eight points form our pharmacophore, although only three of them are considered as essential. Four are pharmacophoric points coming from Leu^{82} and Leu^{83} and contain hydrophobic and hydrogen bond acceptor (carbonyl oxygen). Asp^{80} is involved in hydrogen bonds that have been identified experimentally. Asp^{85} and Arg^{84} although not having importance from an experimental point of view, have been included in coherence with our theoretical results. All these residues are located in the DxL motif. Residue Ile^{87} is located between the DxL motif and the h1h2 loop. Fig. 9 shows the spatial distribution of points belonging to this suggested pharmacophore for TACI–APRIL complex.

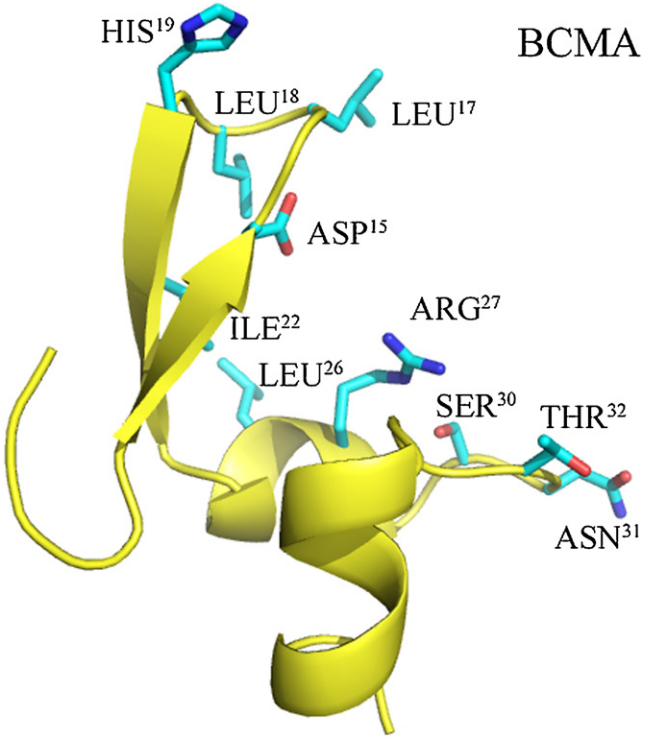

Fig. 8. Spatial representation of the important BCMA residues to bind APRIL.

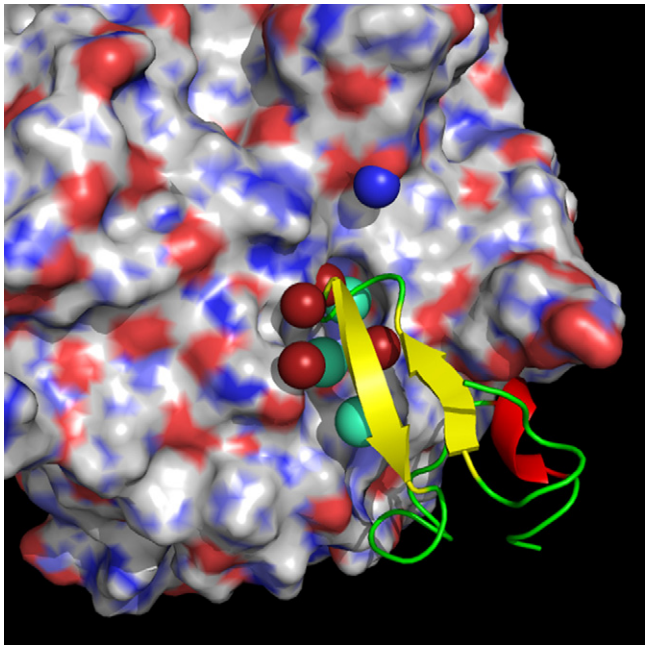

Fig. 9. Spatial representation of the selected pharmacophoric points. In colour cyan the hydrophobic points, in red the hydrogen acceptors and in blue the hydrogen donor.

The suggested pharmacophore for the BCMA–APRIL complex is very similar to that of the TACI–APRIL complex in the DxL region, with the exception of Arg^{84} that in BCMA is mutated to His^{19}. Also Asp^{85} disappears because of its mutation to Ala^{20}. Finally Arg^{27} (Ile^{92} in TACI), far away from the DxL motif, appears as important.

4. Conclusions

Molecular dynamics simulations of the APRIL–TACI/BCMA complexes were performed with the aim to achieve a better understanding of the hydrogen bond, van der Waals and electrostatic contacts of both proteins. As expected, most interactions already observed in NMR or crystal structure were conserved through the MD simulation. However, the simulation showed small differences in hydrogen bonds and some other important residues like Arg^{84} in TACI. As the results for murine and human APRIL complexes have practically the same important residues we can suggest a pharmacophore to obtain new inhibitor for APRIL. Thus, three points on DxL motif were selected to be essential pharmacophoric points and

there were five points more that have been defined as not essential. All those points are located on the DxL motif with the exception of Ile^{87} that is located in h1h2 loop.

In summary, the present work can be considered as a first step in the modelling of drugs mimicking hAPRIL–TACI/BCMA complexes. Due to the small contact surface between both proteins, we think that it could be possible to design a drug, with low molecular weight, capable of embracing the main interactions deduced from the MD simulation.

Acknowledgements

The work was supported by Ministerio Español de Ciencia y Tecnologia (project CTQ2011-29285-C02-02) and the Generalitat de Catalunya (project 2009SGR1308).

Appendix A. Supplementary data

Supplementary data associated with this article can be found, in the online version, at http://dx.doi.org/10.1016/j.jmgm.2012.11.002.

References

[1] M. Hahne, T. Kataoka, M. Schröter, K. Hofmann, M. Irmler, J.L. Bodmer, P. Schneider, T. Bornand, N. Holler, L.E. French, B. Sordat, D. Rimoldi, J. Tschopp, APRIL, a new ligand of the tumor necrosis factor family, stimulates tumor cell growth, Journal of Experimental Medicine 188 (1998) 1185–1190.
[2] C. Bossen, P. Schneider, BAFF, APRIL and their receptors: structure, function and signaling, Seminars in Immunology 18 (2006) 263–275.
[3] J. Hendriks, L. Planelles, J. de Jong-Odding, G. Hardenberg, S.T. Pals, M. Hahne, M. Spaargaren, J.P. Medema, Heparan sulfate proteoglycan binding promotes APRIL-induced tumor cell proliferation, Cell Death and Differentiation 12 (2005) 637–648.
[4] K. Ingold, A. Zumsteg, A. Tardivel, B. Huard, Q.G. Steiner, T.G. Cachero, F. Qiang, L. Gorelik, S.L. Kalled, H. Acha-Orbea, P.D. Rennert, J. Tschopp, P. Schneider, Identification of proteoglycans as the APRIL-specific binding partners, Journal of Experimental Medicine 201 (2005) 1375–1383.
[5] A. Hatzoglou, J. Roussel, M.F. Bourgeade, E. Rogier, C. Madry, J. Inoue, O. Devergne, A. Tsapis, TNF receptor family member BCMA (B cell maturation) associates with TNF receptor-associated factor (TRAF) 1, TRAF2, and TRAF3 and activates NF-kappa B, elk-1, c-Jun N-terminal kinase, and p38 mitogen-activated protein kinase, Journal of Immunology 165 (2000) 1322–1330.
[6] H.M. Kim, K.S. Yu, M.E. Lee, D.R. Shin, Y.S. Kim, S.G. Paik, O.J. Yoo, H. Lee, J.O. Lee, Crystal structure of the BAFF–BAFF–R complex and its implications for receptor activation, Natural Structural Biology 10 (2003) 342–348.
[7] S.R. Dillon, J.A. Gross, S.M. Ansell, A.J. Novak, An APRIL to remember: novel TNF ligands as therapeutic targets, Nature Reviews Drug Discovery 5 (2006) 235–246.
[8] Z. Liu, A. Davidson, BAFF inhibition: a new class of drugs for the treatment of autoimmunity, Experimental Cell Research 317 (2011) 1270–1277.
[9] D. Wang, Y. Chang, Y. Wu, L. Zhang, S. Yan, G. Xie, Q. Qin, J. Jin, W. Wang, J. Fang, W. Wei, Therapeutic effects of TACI-Ig on rat with adjuvant arthritis, Clinical and Experimental Immunology 163 (2011) 225–234.
[10] L. Planelles, S. Castillo-Gutiérrez, J.P. Medema, A. Morales-Luque, H. Merle-Béral, M. Hahne, APRIL but not BLyS serum levels are increased in chronic lymphocytic leukemia: prognostic relevance of APRIL for survival, Haematologica 92 (2007) 1284–1285.
[11] C. Kern, J.F. Cornuel, C. Billard, R. Tang, D. Rouillard, V. Stenou, T. Defrance, F. Ajchenbaum-Cymbalista, P.Y. Simonin, S. Feldblum, J.P. Kolb, Involvement of BAFF and APRIL in the resistance to apoptosis of B-CLL through an autocrine pathway, Blood 103 (2004) 679–688.
[12] M. Abe, S. Kido, M. Hiasa, A. Nakano, A. Oda, H. Amou, T. Matsumoto, BAFF and APRIL as osteoclast-derived survival factors for myeloma cells: a rationale for TACI-Fc treatment in patients with multiple myeloma, Leukemia 20 (2006) 1313–1315.
[13] P. Mhawech-Fauceglia, G. Kaya, G. Sauter, T. McKee, O. Donze, J. Schwaller, B. Huard, The source of APRIL up-regulation in human solid tumor lesions, Journal of Leukocyte Biology 80 (2006) 697–704.
[14] G.A.R. Young, H.J. Iland, Clinical perspectives in lymphoma, Internal Medicine Journal 37 (2007) 478–484.
[15] T. Koyama, H. Tsukamoto, K. Masumoto, D. Himeji, K. Hayashi, M. Harada, T. Horiuchi, A novel polymorphism of the human APRIL gene is associated with systemic lupus erythematosus, Rheumatology 42 (2003) 980–985.
[16] V. Hornak, R. Abel, A. Okur, B. Strockbine, A. Roitberg, C. Simmerling, Comparison of multiple Amber force fields and development of improved protein backbone parameters, Proteins: Structure, Function, and Bioinformatics 65 (2006) 712–725.
[17] D.A. Case, T.A. Darden, T.E. Cheatham III, C.L. Simmerling, J. Wang, R.E. Duke, R. Luo, R.C. Walker, W. Zhang, K.M. Merz, B.P. Roberts, B. Wang, S. Hayik, A. Roitberg, G. Seabra, I. Kolossváry, K.F. Wong, F. Paesani, J. Vanicek, J. Liu, X. Wu, S.R. Brozell, T. Steinbrecher, H. Gohlke, Q. Cai, X. Ye, J. Wang, M.-J. Hsieh, G. Cui, D.R. Roe, D.H. Mathews, M.G. Seetin, C. Sagui, V. Babin, T. Luchko, S. Gusarov, A. Kovalenko, P.A. Kollman, AMBER 11, University of California, San Francisco, 2010.
[18] T. Darden, D. York, L. Pedersen, Particle mesh Ewald: an $N\log(N)$ method for Ewald sums in large systems, The Journal of Chemical Physics 98 (1993) 10089–10092.
[19] W.L. Jorgensen, J. Chandrasekhar, J.D. Madura, R.W. Impey, M.L. Klein, Comparison of simple potential functions for simulating liquid water, The Journal of Chemical Physics 79 (1983) 926–935.
[20] P.A. Kollman, I. Massova, C. Reyes, B. Kuhn, S. Huo, L. Chong, M. Lee, T. Lee, Y. Duan, W. Wang, O. Donini, J. Srivasan, D.A. Case, T.E. Cheatam 3rd, Calculating structures and free energies of complex molecules: combining molecular mechanics and continuum models, Accounts of Chemical Research 33 (2000) 889–897.
[21] W. Humphrey, A. Dalke, K. Schulten, VMD: visual molecular dynamics, Journal of Molecular Graphics 14 (1996) 33–38.
[22] S.G. Hymowitz, D.R. Patel, H.J.A. Wallweber, S. Runyon, M. Yan, J. Yin, S.K. Shriver, N.C. Gordon, B. Pan, N.J. Skelton, R.F. Kelley, M.A. Starovasnik, Structures of APRIL–receptor complexes: like BCMA, TACI employs only a single cysteine-rich domain for high affinity ligand binding, Journal of Biological Chemistry 280 (2005) 7218–7227.
[23] H.J.C. Berendsen, J.P.M. Postma, W.F. van Gunsteren, A. DiNola, J.R. Haak, Molecular dynamics with coupling to an external bath, The Journal of Chemical Physics 81 (1984) 3684–3690.
[24] J.P. Ryckaert, G. Ciccotti, H. Berendsen, Numerical integration of the Cartesian equations of motion of a system with constraints: molecular dynamics of n-alkanes, Journal of Computational Physics 23 (1997) 327–341.
[25] A. Onufriev, D. Bashford, D.A. Case, Exploring protein native states and large-scale conformational changes with a modified generalized Born model, Proteins 55 (2004) 383–394.
[26] R.A. Laskowski, J.A. Rullmannn, M.W. MacArthur, R. Kaptein, J.M. Thornton, AQUA and PROCHECK-NMR: programs for checking the quality of protein structures solved by NMR, Journal of Biomolecular NMR 8 (1996) 477–486.
[27] H.J.A. Wallweber, D.M. Compaan, M.A. Starovasnik, S.G. Hymowitz, The crystal structure of a proliferation-inducing ligand, APRIL, Journal of Molecular Biology 343 (2004) 283–290.